Chinese Chemical Letters 33 (2022) 1861–1864

Contents lists available at ScienceDirect

Chinese Chemical Letters

journal homepage: www.elsevier.com/locate/cclet

The exquisite integration of ESIPT, PET and AIE for constructing fluorescent probe for Hg(II) detection and poisoning

Xiang Cheng[a,b,c], Shuai Huang[a,b,c], Qian Lei[a,b,c], Fei Chen[a,b,c], Fan Zheng[a,b,c], Shibo Zhong[a,b,c], Xueyan Huang[a,b,c], Bin Feng[a,b,c], Xueping Feng[d], Wenbin Zeng[a,b,c,*]

[a] Xiangya School of Pharmaceutical Sciences, Central South University, Changsha 410013, China
[b] The Molecular Imaging Research Center, Central South University, Changsha 410013, China
[c] Hunan Key Laboratory of Diagnostic and Therapeutic Drug Research for Chronic Diseases, Central South University, Changsha 410013, China
[d] Xiangya Hospital, Central South University, Changsha 410013, China

ARTICLE INFO

Article history:
Received 21 August 2021
Revised 30 September 2021
Accepted 11 October 2021
Available online 16 October 2021

Keywords:
Aggregation-induced emission
Excited state intramolecular proton transfer
Photoinduced electron transfer
Mercury ions
Fluorescent imaging

ABSTRACT

Excessive mercury ions (Hg^{2+}) in the environment can accumulate in human body along with the food chain to cause serious physiological reactions. The fluorescence probes were considered as convenient tool with great potential for Hg^{2+} detection. Most existing probes suffer from aggregation-induced quenching (ACQ) effects and insufficient sensitivity. Herein, a novel type of fluorophore was developed by combining the aggregation-induced emission (AIE) and excited state intramolecular proton transfer (ESIPT) characteristics. Subsequently, a phenyl thioformate group with photoinduced electron transfer (PET) effect was connected to give an efficient "turn-on" probe (HTM), which exhibited good selectivity toward Hg^{2+}, short response time (30 min), coupled with extremely low detection limit (LOD = 1.68 nmol/L). In addition, HTM was used successfully in real samples, cells and drug evaluation, underlying the superiority of HTM to detect Hg^{2+} in practical applications.

Toxic metal pollution has emerged as an increasingly concerned problem [1,2] due to the deleterious effects on nature, environment [3], food security, and human health [4]. Mercury is a kind of heavy metal that exists in different forms, including elementary, inorganic, and organic form [5]. The toxicity of mercury on health was depended on different existent forms and exposure pathways [6]. As Hg^{2+} possesses the ability to form stable complexes with amino acids containing sulfur [7], it can cause the structure and function disorder in cells thereby leading to serious diseases linked to neurotoxicity [8], hepatotoxicity [9], and nephrotoxicity [10]. Nevertheless, mercury is still widely utilized in many industrial processes [11]. Thus, there are urgent needs for developing a method enabling of detecting and quantifying mercury ions both in environmental and biological samples with high efficiency, sensitivity, and instantaneity [12].

Traditional analytical techniques for mercury ions include spectrophotometry, atomic absorption spectroscopy, X-ray absorption spectroscopy, atomic fluorescence spectroscopy, and inductively coupled plasma mass spectrometry [13–15]. But none of them could achieve in-situ real-time monitoring, even sometimes they may bring destruction to biological samples [16–18]. Fluoroscopy, as one of the most popular methods [19], possessing numerous advantages including low cost [20], good selectivity [21], high sensitivity [22,23], rapid responsiveness [24] and real-time monitoring [25,26]. Fluorescent probes can be mainly classified as two types. One is based on reversible Lewis acid-base combination fluorescent probes [27–29], signal-decreased fluorescent probes [30], and ratio metric fluorescent probes [31], the other type is based on specific chemical reactions promoted by Hg^{2+} such as rhodamine ring-opening reaction [9], desulfurization [32], deprotection of thioacetals [33], nitrogen-complex reaction [6], hydrolysis. Nevertheless, the most existing fluorescent probes still have many limitations such as complicated organic synthesis, low sensitivity and selectivity, inefficiency in water, perturbation from endogenous active species, turn-off response. Hence, developing a novel fluorescent probe to efficiently detect Hg^{2+} with optimized performance including strong anti-interference ability, good application in aqueous solution and turn-on response to avoid such disadvantages is particularly important. So far, some Hg^{2+} recognition sites have been reported. Among them, phenyl thiochloroformate has attracted the most attention because of its high sensitivity, strong specificity and fast response speed.

* Corresponding author.
E-mail address: wbzeng@hotmail.com (W. Zeng).

https://doi.org/10.1016/j.cclet.2021.10.024
1001-8417/

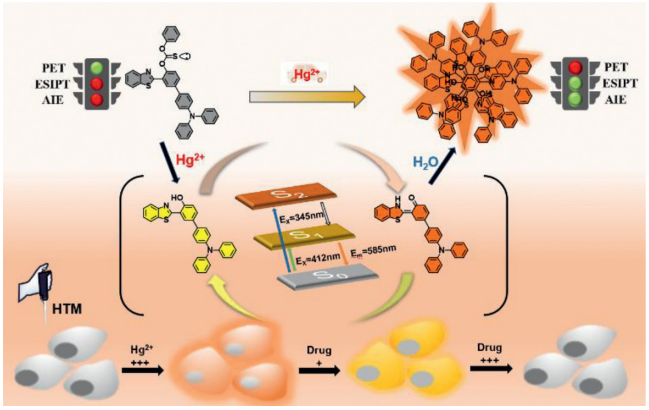

Scheme 1. Schematic illustration of proposed mechanism of probe HTM to Hg^{2+}, construction and theoretical insight studies with the ESIPT fluorescent probe, and HTM application in cell imaging and drug evaluation.

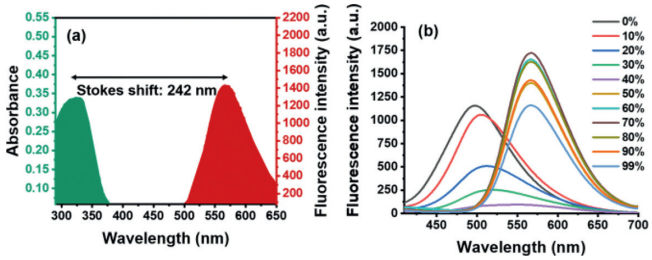

Fig. 1. (a) Stokes shift of HTM. (b) The fluorescence emission spectra of HTO in different DMSO-H_2O mixtures.

In this work, we designed a new type of "turn-on" small molecule fluorescent probe HTM combining PET, ESIPT and AIE effects for the sensitive, specific detection of Hg^{2+}. In our strategy, a novel excited-state intramolecular proton-transfer (ESIPT) fluorophore (HTO) was integrated with aggregation induced emission (AIE) feature *via* the introduction of triphenylamine. It not only extended the π-conjugation and led to red shift of the emission wavelength, but also took full advantage of AIE effect to acquire remarkable ability in the aqueous environment. Further, a Hg^{2+} specific small molecule fluorescent probe HTM was obtained through intermolecular reaction between phenyl chlorothionocarbonate and HTO. Due to the photoinduced electron transfer (PET) of the phenyl thioformate and the substitution of hydroxyl hydrogen, the ESIPT process was blocked, resulting in the fluorescence quenching. Upon addition of Hg^{2+}, due to the high affinity of mercury toward sulfur atoms, the ester bond was broken and mercury sulfide was released, thereby restoring the ESIPT process with simultaneous destruction of PET process to reactivate the fluorescence (Scheme 1). Besides, we used density functional theory (DFT) and time-dependent density functional theory (TD-DFT) to conduct an in-depth study on the fluorescence mechanism of the probe's ESIPT system. Importantly, the probe had the advantages of a large Stokes shift 242 nm (Fig. 1a) and a low detection limit. Additionally, HTM was successfully used for the detection of mercury ions in actual water samples, food and living cells, last but not least, the probe was successfully used to evaluate clinical therapeutic drugs for mercury poisoning.

In the palladium catalyst-mediated Suzuki cross coupling reaction, incorporating 2-(2′-hydroxyphenyl)benzothiazole (HBT) into the triphenylamine (TPA) to obtain the chromophore with both AIE and ESIPT properties. Finally, PET was successfully integrated into the AIE and ESIPT fluorophore through the tandem connection of phenyl thiochloroformate and chromophore. The detailed synthetic routes of HTM were described in the Scheme S1 (Supporting information).

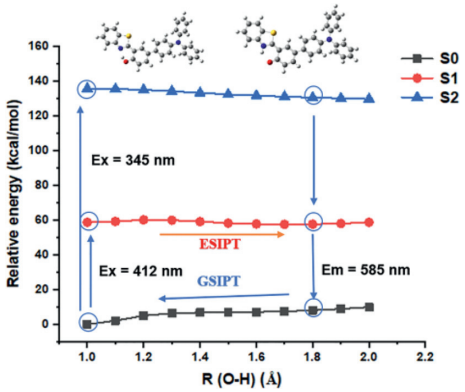

Fig. 2. (a) The HTO (PBE0/def2-SVP)-optimized S1 energy and S2 energy profiles along the O–H distances.

Then, we studied the AIE characteristics of HTO in the DMSO/water mixture with different water fractions (fw) (Fig. 1b). In pure DMSO solution showed green fluorescence which was assigned to enol emission. With increasing of water percentage to 40% the fluorescence intensity had a remarkable decrease at 567 nm (Fig. S2a in Supporting information). The phenomenon could be ascribed to the ESIPT effect was more pronounced at a lower water content. As the fraction of water elevated, the hydroxyl hydrogen was easy to leave, and the enol tautomerism in the molecule led to energy consumption through non-radiative transitions. As the fw was reached 70%, the fluorescence intensity at 567 nm increased greatly. It can be ascribed to the AIE effect caused by the aggregation of HTO in the poor solvent that showing intensive. As the fw was above 70%, the drop of fluorescence could be explained by the fact that the change in the aggregation state of HTO, which made the molecular movement increase and the fluorescence intensity decrease [34]. Combined with the above solvation behavior, this novel fluorophore exhibited unique properties. Concretely, it showed AIE performance at the keto emission location in aggregation state, while only enol emission in the solution owing to the high energy barrier.

To better understand the fluorescent emission mechanism of HTM and HTO, DFT and TD-DFT calculation was performed based on the level of PBE0/Def2-svp. For the study of the ESIPT properties of HTO as shown in Fig. 2, it suggested that after being excited, the enol molecule in the S1 state experiences an energy barrier 1.43 kcal/mol and enable the ESIPT process. The solvent effect was studied to interpret the double peaks of the enol and ketones. According to the electron hole analysis (Figs. S3a-c in Supporting information) [35], both HTM and HTO are typical charge transfer excitations. The formation of the O-state in the solvent effect is consistent with the effect in the alkaline environment, so a single peak appears at 500 nm. According to the calculation, the oscillator strength of HTM is 0.0644, which implies that the probability of transition is very small and the probability of fluorescence emission is very low. This shows that the weak fluorescence emission of the probe is indeed affected by PET, which is consistent with the experimental results.

To study the response to Hg^{2+}, we firstly investigated the response time of the probe (Fig. 3a). The response of HTM towards different concentrations of Hg^{2+} showed that the fluorescence intensity reached maximum within 30 min. The results reflected a fast response of the probe to Hg^{2+}. Secondly, we studied the linear response of Hg^{2+}. Through the fluorescence titration experiment, the changes in the fluorescence spectrum were record upon incubation with different concentrations of Hg^{2+} (0–1000 nmol/L) (Fig. 3b). From 10 nmol/L to 1000 nmol/L, the fluorescence intensity at 567 nm kept increasing, indicating HTM can work as a

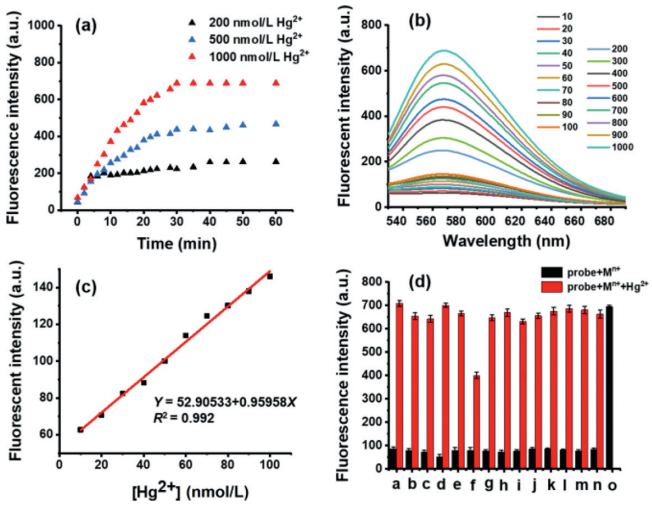

Fig. 3. (a) The relationship between the fluorescence intensity of HTM (10 μmol/L) and the reaction time with different concentrations of Hg^{2+}. (b) The fluorescence spectrum of HTM after adding different concentrations of Hg^{2+} (10–1000 nmol/L). (c) The linear fit curve of HTM fluorescence intensity with 10–100 nmol/L. (d) Fluorescence responses of HTM (10 μmol/L) toward other substances (100 μmol/L) and Hg^{2+} (1 μmol/L): a: Ag^{2+}, b: Al^{3+}, c: As^{3+}, d: Cd^{2+}, e: Cs^{2+}, f: Cu^{2+}, g: Fe^{2+}, h: K^{+}, i: Mg^{2+}, j: Mn^{2+}, k: Na^{+}, l: Ni^{2+}, m: Pd^{2+}, n: Zn^{2+}. λ_{ex} = 365 nm, λ_{em} = 567 nm.

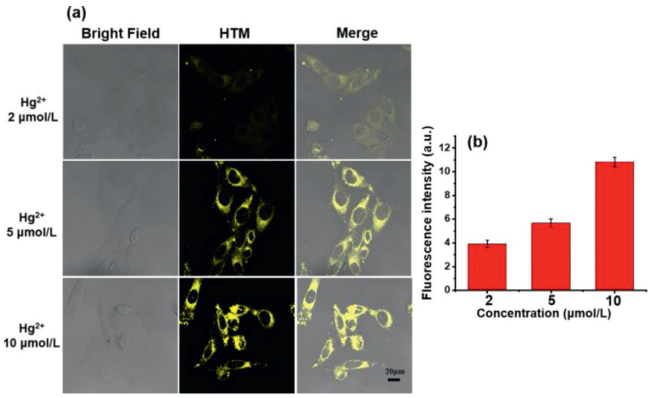

Fig. 4. (a) The HepG2 cell imaging of HTM (10 μmol/L) with different concentrations of Hg^{2+} after incubation for 30 min. Yellow channel (λ_{ex} = 405 nm, collected at 550–600 nm, scale bar: 20 μm). (b) The fluorescent intensity of HTM with the different concentrations of Hg^{2+}.

"turn-on" fluorescent probe for Hg^{2+} detection. Moreover, excellent linearity was observed in this concentration range (R^2 = 0.993) (Fig. S4a in Supporting information). To further investigate the potential of HTM in practical applications, the response ability of the probe towards a lower concentration of Hg^{2+} was carried out. As can be seen from Fig. 3c, even if Hg^{2+} was at an extremely low concentration of 0–100 nmol/L, HTM still had an excellent linear relationship (R^2 = 0.992). It revealed that HTM had a great detection ability for tracing Hg^{2+}. Subsequently, according to $3\sigma/k$ (the ratio of the standard deviation of the triple blank sample to the slope of the linear equation), the detection limit was calculated to be 1.68 nmol/L, which is much lower than the allowed level of 2 ppb (about 10 nmol/L) in drinking water by US Environmental Protection Agency [36]. Compared with most other reported probes (Table S1 in Supporting information), HTM behave as a "turn-on" Hg^{2+} fluorescent probe with a better linear response and a lower detection limit.

Taking into account of the diversity of the detection environment, we also studied the fluorescence changes of HTM with or without Hg^{2+} in a wide pH range. As shown in Fig. S5 (Supporting information), it revealed that the probe was in good stability, could display a good response in a wide range of pH (pH 5–10), and had the potential to be used in a variety of environments to track Hg^{2+}. In order to further investigate the Hg^{2+} sensing ability of HTM in a complex detection environment, the selectivity and anti-interference of HTM to Hg^{2+} were explored (Fig. 3d). The fluorescence intensity of HTM was not basically influenced by 10 equiv. of other analytes including Na^{+}, Ca^{2+}, Fe^{2+}, Al^{3+}, Mn^{2+}, Ag^{+}, Cd^{2+}, K^{+}, Mg^{2+}, Zn^{2+}, CS^{+}, Cu^{2+}, Ni^{2+}, As^{3+}, and Pd^{2+}. Only in the exist of Hg^{2+}, the fluorescence signal was intensively enhanced at 567 nm (Fig. S4b in Supporting information). The results implied that HTM had favorable selectivity and anti-interference ability. Although Cu^{2+} had a certain quenching effect on the probe, it did not affect the specific detection of Hg^{2+}. These results suggested that HTM may have the capability of specifically and sensitively detecting Hg^{2+} in a complex environment.

To further verify the potential response mechanism of HTM to Hg^{2+}, a high-performance liquid chromatography (HPLC) analysis was performed. As depicted in Fig. S6 (Supporting information), the retention times of HTM and HTO were 10.04 min and 11.47 min, respectively. When 0.5 equiv. of Hg^{2+} was added to HTM, the peak of HTO appeared. Later, the mechanism was verified by high-resolution mass spectrometry in Fig. S7 (Supporting information). Moreover, HTO molecules self-assembled into nanoparticles with a size of 190 nm (Fig. S8 in Supporting information) and the emission was enhanced due to the AIE effect.

Considering the results obtained from the above experiments, HTM presents the advantages of good selectivity, strong anti-interference ability, low detection limit and good detection linearity for tracing Hg^{2+}. We then investigated the potential of HTM to detect Hg^{2+} in complex real samples including seafood, drinks and river water. As shown in Fig. S9 (Supporting information), the growing fluorescence intensity at 567 nm had a good linearity with the increasing concentration of Hg^{2+} (100–1000 nmol/L) in complex samples. It indicated that HTM could detect low concentrations of Hg^{2+} in actual samples. As shown in Table 1, the calculated recovery rate of Hg^{2+} was 91.3%–110.0%, and the relative error was less than 10%. These results demonstrated that HTM was feasible for the detection of Hg^{2+} in complex matrixes, suggesting its great potential in real-world environmental and biochemical detection.

Before the application in living cells, for the safety concerns, the cytotoxicity of HTM against HepG2 cells was evaluated. As depicted in Fig. S10 (Supporting information), the results showed that the probe had low cytotoxicity. Whereafter, we further investigated the imaging capability of the probe at a cellular level. HepG2 cells were incubated only with 10 μmol/L HTM at first. No fluorescence showed up in 30 min co-incubation (Fig. S11 Supporting information). Upon the addition of Hg^{2+} (2–10 μmol/L), the yellow fluorescence was turned on (Fig. 4). Notably, the fluorescence signal increased in a dose-dependent manner (Fig. 4b). The scavenging ability of DMPS [37] (sodium dimercaptosulphonate) towards the mercury ion was also evaluated. DMPS was an antidote for Hg^{2+} poisoning which was commonly used in clinical practice. As DMPS was added, the fluorescence signal from the yellow channel decreased. Besides, the fluorescence intensity decreased along with the growing concentration of DMPS (Fig. 5). When the same amount of DMPS and Hg^{2+} were added, the fluorescence was barely observed. The fluorescence signal showed two opposite dose-dependences for Hg^{2+} and DMPS, and they corresponded to each other. The above results undeniably demonstrated the ability of probe to evaluate DMPA for Hg^{2+} poisoning in living cells which granted it the potential of clinicopathological analysis. These results demonstrated HTM as an effective imaging probe for the detection of Hg^{2+} in cells.

In summary, we have constructed a "turn-on" fluorescent probe HTM for $Hg^{2+}$with high sensitivity in extensive matrixes. We de-

Table 1
Application of HTM in determination of Hg^{2+} in actual samples.

Sample	Found (μmol/L)	Added (μmol/L)	Found (μmol/L)	Recovery (%)	Relative error (%)
Octopus	ND	0.5	0.53 ± 0.02	106.0	6.0
		0.8	0.78 ± 0.04	97.5	2.5
		1.0	1.01 ± 0.01	101.0	1.0
Fish	ND	0.5	0.53 ± 0.04	106.0	6.0
		0.8	0.76 ± 0.05	95.0	5.0
		1.0	1.01 ± 0.01	101.0	1.0
Shrimp	ND	0.5	0.53 ± 0.05	106.1	6.0
		0.8	0.73 ± 0.04	91.3	8.7
		1.0	1.05 ± 0.05	105.0	5.0
Pearl River	ND	0.5	0.49 ± 0.02	98.0	2.0
		0.8	0.74 ± 0.02	92.5	7.5
		1.0	1.06 ± 0.03	106.0	6.0
Drink	ND	0.5	0.48 ± 0.04	96.0	4.0
		0.8	0.74 ± 0.02	92.5	7.5
		1.0	1.05 ± 0.02	105.0	5.0
Xiangjiang River	ND	0.5	0.55 ± 0.01	110.0	10.0
		0.8	0.79 ± 0.01	98.8	1.2
		1.0	0.97 ± 0.01	97.0	3.0

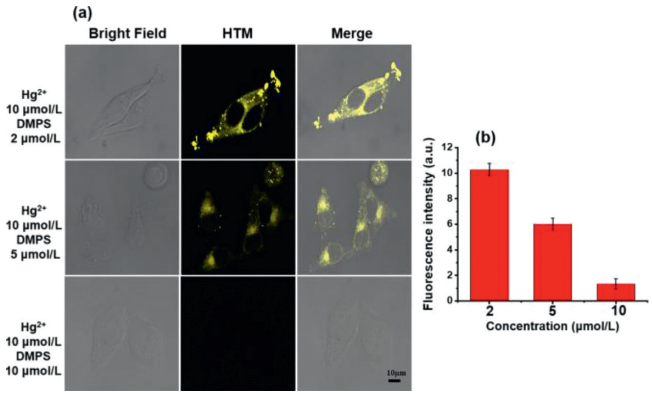

Fig. 5. (a) HepG2 cells containing different concentrations (2.0, 5.0 and 10 μmol/L) of DMPS and Hg^{2+} (10 μmol/L) were incubated for 40 min and then HTM (10 μmol/L) cells were added for imaging. Yellow channel (λ_{ex} = 405 nm, collected at 550–600 nm, scale bar: 10 μm). (b) The fluorescent intensity of HTM with the different concentrations of DMPS.

signed an ESIPT-type fluorophore HTO with AIE effect through a simple synthesis method, and then introduced phenyl thioformate group as a recognition site toward Hg^{2+}. Due to the PET process from sulfur atom to fluorophore, interference of background can be reduced significantly. Upon activation by Hg^{2+}, the fluorescence intensity at 567 nm intensified abundantly and more notably, the probe has a preferable anti-interference ability, and achieves sensational linear detection at the nanomolar level (LOD = 1.68 nmol/L). Further application of the probe in real water samples, seafood samples, living cells and evaluating clinical therapeutic drugs of mercury ions demonstrated the substantial potential of HTM in detecting and tracing of Hg^{2+} in low concentration. These results suggest that probe HTM can be a valuable tool for monitoring Hg^{2+} in a variety of complex environments.

Declaration of competing interest

The authors declare that they have no known competing financial interests or personal relationships that could have appeared to influence the work reported in this paper

Acknowledgments

We are grateful for the financial supports from the National Natural Science Foundation of China (Nos. 81971678 and 81671756) and the Innovation Fund for Post graduate Students of Central South University (No. 2020zzts827).

Supplementary materials

Supplementary material associated with this article can be found, in the online version, at doi:10.1016/j.cclet.2021.10.024.

References

[1] N. Ferreira-Rodriguez, A.J. Castro, B.N. Tweedy, et al., J. Environ. Manage. 282 (2021) 111528–111535.
[2] N.E. Selin, Science 360 (2018) 607–609.
[3] L.T. Budnik, L. Casteleyn, Sci. Total. Environ. 654 (2019) 720–734.
[4] L. Yang, Y. Zhang, F. Wang, et al., Chemosphere 245 (2020) 125586–125620.
[5] Q. Wang, D. Kim, D.D. Dionysiou, et al., Environ. Pollut. 131 (2004) 323–336.
[6] Q. Fu, X. Fan, J. Sun, et al., Small 16 (2020) e2000072.
[7] O.P. Ajsuvakova, A.A. Tinkov, M. Aschner, et al., Coord. Chem. Rev. 417 (2020) 213343–213359.
[8] H.H. Harris, I.J. Pickering, G.N. George, Science 301 (2003) 1203.
[9] F.Y. Yan, D.L. Cao, N. Yang, et al., Sens. Actuators B: Chem. 162 (2012) 313–320.
[10] Z. Khoshbin, M.R. Housaindokht, A. Verdian, et al., Biosens. Bioelectron. 116 (2018) 130–147.
[11] P. Mahato, A. Ghosh, S. Saha, et al., Inorg. Chem. 49 (2010) 11485–11492.
[12] L. Zhao, Z. Zhang, Y. Liu, et al., J. Hazard. Mater. 385 (2020) 121556–121564.
[13] Y. Jiang, H. Li, R. Chen, et al., Spectrochim. Acta A: Mol. Biomol. Spectrosc. 251 (2021) 119438–119446.
[14] Y. Wang, L. Zhang, X. Han, et al., Chem. Eng. J. 406 (2021) 127166–127180.
[15] H. Erxleben, J. Ruzicka, Anal. Chem. 77 (2005) 5124–5128.
[16] L. Wu, A.C. Sedgwick, X. Sun, et al., Acc. Chem. Res. 52 (2019) 2582–2597.
[17] H. Ren, F. Huo, Y. Huang, et al., Dyes Pigm. 181 (2020) 108567–108573.
[18] H. Ren, F. Huo, X. Wu, et al., Chem. Commun. (Camb) 57 (2021) 655–658.
[19] Y. Wen, F. Huo, C. Yin, Chin. Chem. Lett. 30 (2019) 1834–1842.
[20] H. Ren, F. Huo, Y. Zhang, et al., Sens. Actuators B: Chem. 319 (2020) 128248–128255.
[21] B. Zhang, H. Zhang, M. Zhong, et al., Chin. Chem. Lett. 31 (2020) 133–135.
[22] B. Feng, Y. Zhu, J. Wu, et al. , Chin. Chem. Lett. 32 (2021) 3057–3060.
[23] X. Yang, W. Liu, J. Tang, et al., Chem. Commun. (Camb) 54 (2018) 11387–11390.
[24] H. Zhang, P. Xu, X. Zhang, et al., Chin. Chem. Lett. 31 (2020) 1083–1086.
[25] A. Bi, M. Liu, S. Huang, et al., Chem. Commun. (Camb) 57 (2021) 3496–3499.
[26] L. Huang, X. Cao, T. Gao, et al., Talanta 225 (2021) 121950–121956.
[27] S. Yoon, A.E. Albers, A.P. Wong, et al., J. Am. Chem. Soc. 127 (2005) 16030–16031.
[28] B. Zhou, S. Qin, B. Chen, et al., Tetrahedron Lett. 59 (2018) 4359–4363.
[29] S. Erdemir, O. Kocyigit, Dyes Pigm. 145 (2017) 72–79.
[30] S. Gharami, K. Aich, P. Ghosh, et al., Dalton Trans. 49 (2020) 187–195.
[31] S. Das, A. Sarkar, A. Rakshit, et al., Inorg. Chem. 57 (2018) 5273–5281.
[32] S. Huang, T. Gao, A. Bi, et al., Dyes Pigm. 172 (2020) 107830–107838.
[33] T. Gao, X. Huang, S. Huang, et al., J. Agric. Food Chem. 67 (2019) 2377–2383.
[34] Y. Tu, Y. Yu, D. Xiao, et al., Adv. Sci. 7 (2020) 2001845.
[35] T. Lu, F.W. Chen, J. Comput. Chem. 33 (2012) 580–592.
[36] G.H. Chen, W.Y. Chen, Y.C. Yen, et al., Anal. Chem. 86 (2014) 6843–6849.
[37] C.C. Bridges, L. Joshee, R.K. Zalups, Toxicol. Sci. 105 (2008) 211–220.